Springer

KSME

Journal of Mechanical Science and Technology 24 (10) (2010) 2051~2057
www.springerlink.com/content/1738-494x
DOI 10.1007/s12206-010-0620-0

Heat-transfer analysis of indirect moxibustion using unsteady conjugate heat-transfer solutions †

Byoung Jin Jeon[1] and Hyoung Gwon Choi[2*]

[1]*Department of Energy System, Graduate School of Energy and Environment, Seoul National University of Technology, 172 Gongreung-2-Dong, Nowon-Gu, Seoul 139-743, Republic of Korea*
[2]*Department of Mechanical Engineering, Seoul National University of Technology, 172 Gongreung-2-Dong, Nowon-Gu, Seoul 139-743, Republic of Korea*

(Manuscript Received February 19, 2010; Revised May 18, 2010; Accepted June 13, 2010)

Abstract

A conjugate heat-transfer problem in indirect moxibustion was analyzed by solving the problem of unsteady convective heat transfer coupled with conductive heat transfer. The interaction of a combustion-heated paper disk of moxa with the body and surrounding fluid was revealed by examining the body's unsteady temperature distributions. From the grid- and time step-independent solutions to the present conjugate heat-transfer problem, the effective stimulation periods for four widths of paper disk, along with the depths of the effective stimulation zones, were obtained. Further, it was found that the effective stimulation zone becomes larger and lasts longer for the wider paper disks, whereas the depth of the effective stimulation zone is saturated beyond a certain size. Lastly, the streamline pattern and the history of the spatially averaged heat-transfer coefficient, which is related to the convective heat transfer between the body and the surrounding fluid, were determined.

Keywords: Conjugate heat transfer; Moxibustion; Moxa; Effective stimulation zone

1. Introduction

Moxibustion therapy is a type of thermal and chemical stimulation involving cauterization of moxa adhered to the skin of a patient [1]. Although it has been shown to be effective for various diseases and pains, it is not yet a fully accepted therapy, due to side-effects such as skin-burning and pain as well as the arbitrariness of its procedure [2]. Therefore, in order to eliminate those drawbacks, recent research on moxibustion therapy has focused more on the scientific aspects of the methodology than was the case previously.

In order to quantitatively investigate the thermal stimulation effected by moxibustion, accurate accounting for and prediction of its heat transfer to the body are necessary. Many researchers have undertaken experimental studies on the thermal characteristics of moxa combustion. Lee et al. [3-5] tested small and large moxa of different shapes in order to determine the pertinent thermodynamic properties, obtaining data on the combustion time, the temperature gradient and the effective stimulation period. The thermodynamic characteristics of small commercial moxa were determined for the two prevalent shapes using a thermocouple [3]. The lower-density moxa is of cylindrical shape and mounted on a compressed, paper disk with a whole in its center, as shown in Fig. 1, whereas the high-density moxa is of pipe shape and mounted on a hollow cylinder, below which is a hole for combustion. Both cases can be considered to entail indirect moxibustion, since the heat transfer to the skin is carried out through either the paper disk or the air inside the hollow cylinder. Lee et al. [3] found that the high-density moxa was more effective for longer stimulation, and the lower-density one, for shorter, intensive stimulation. Also, they defined the "effective stimulating period," which is the period in which the skin temperature is above that of the body. It should be noted that in their study, moxibustion's heat flux to the body was estimated using the temperatu re difference between the body and the bottom of the moxa, instead of Fourier's law, since the temperature distribution inside the body was not measured. Accordingly, however, strictly quantitative measurement of the heat flux was not possible. Bang et al. [6] and Park et al. [7] analyzed the effect of moxa density on the characteristics of moxibustion. They decomposed the moxibustion cycle into preheating, heating, retaining and cooling periods. They found that the lower the moxa density is, the shorter are the heating and cooling periods, and that the maximum moxa temperature decreases with lower densities. However, in neither of those studies was any

† This paper was recommended for publication in revised form by Associate Editor Dongshin Shin

* Corresponding author. Tel.: +82 -2-970-6312, Fax: +82-2-949-1458
E-mail address: hgchoi@snut.ac.kr

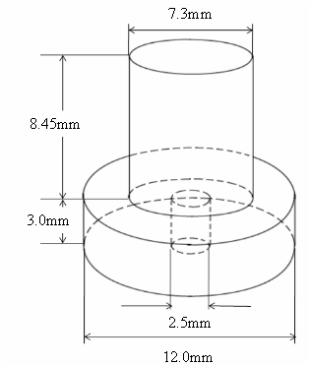

Fig. 1. Schematic of indirect moxa [3].

quantitative measurement of moxibustion's heat flux into the body performed. Zhipeng et al. [8] proposed a heat-transfer model for both direct and indirect moxibustion. But only a simplified conduction model reduced to a simple ordinary differential equation, was derived; the convective heat-transfer mechanism between the moxa and the surrounding fluid was not considered at all.

Compared to the number and variety of the experimental studies on heat transfer in moxibustion, there are, to the present authors' knowledge, only a very few numerical studies on thermal and fluid flow, presumably because the heat-transfer mechanism of moxibustion is so complicated that both conduction and convection are involved, as well as radiation in some cases. Furthermore, experimental investigation of moxibustion has not yet been conducted in any thorough, quantitative way from the viewpoint of conjugate heat transfer. This lacuna in the literature belies the importance of numerical analysis of the conjugate heat-transfer mechanism involved in moxibustion. In the present study, therefore, the solution of unsteady incompressible Navier-Stokes equations was considered in order to directly solve the conjugate heat-transfer problem of moxibustion, particularly the convective heat-transfer mechanism coupled with conductive heat transfer. The unsteady temperature distribution inside the body mainly was investigated, due to its relevance to the effective stimulating period. This paper is organized as follows. In Section 2, the numerical method as well as the boundary condition of the present simulation are briefly introduced. In Section 3, the numerical results obtained from indirect moxibustion are presented and discussed in detail, focusing on the effective thermal stimulation. In Section 4, conclusions are drawn.

2. Numerical method

In the present study's unsteady numerical simulations, a commercial code, ANSYS-Fluent, was used for analysis of axisymmetric incompressible Navier-Stokes equations and energy equations. The governing equations utilized were the following unsteady two-dimensional incompressible Navier-Stokes equations and an energy equation with continuity constraint:

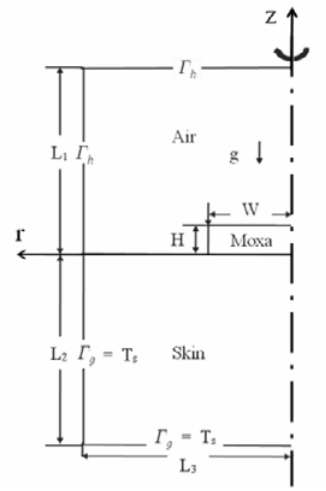

Fig. 2. Schematic of unsteady simulation of conjugate heat transfer.

$$\frac{1}{r}\frac{\partial}{\partial r}(ru_r)+\frac{\partial u_z}{\partial z}=0 \tag{1}$$

$$\rho\left(\frac{\partial u_r}{\partial t}+u_r\frac{\partial u_r}{\partial r}+u_z\frac{\partial u_r}{\partial z}\right) =-\frac{\partial p}{\partial r}+\mu\left(\frac{1}{r}\frac{\partial}{\partial r}\left(r\frac{\partial u_r}{\partial r}\right)+\frac{\partial^2 u_r}{\partial z^2}-\frac{u_r}{r^2}\right)$$
$$\rho\left(\frac{\partial u_z}{\partial t}+u_r\frac{\partial u_z}{\partial r}+u_z\frac{\partial u_z}{\partial z}\right) =-\frac{\partial p}{\partial z}+\mu\left(\frac{1}{r}\frac{\partial}{\partial r}\left(r\frac{\partial u_z}{\partial r}\right)+\frac{\partial^2 u_z}{\partial z^2}\right)+g\rho\beta(T-T_\infty) \tag{2}$$

$$\rho c_v\left(\frac{\partial T}{\partial t}+u_r\frac{\partial T}{\partial r}+u_z\frac{\partial T}{\partial z}\right)=k\left(\frac{1}{r}\frac{\partial}{\partial r}\left(r\frac{\partial T}{\partial r}\right)+\frac{\partial^2 T}{\partial z^2}\right) \tag{3}$$

The SIMPLE algorithm was adopted for unsteady simulation, and the second-order implicit method was used for time marching; turbulence modeling was not considered, as explained below in Section 3. The second-order upwind method was employed for spatial discretization of the convection terms of momentum and energy equations. Fig. 2 shows a schematic of the unsteady simulation of the conjugate heat transfer. The temperature of the body along the boundary Γ_g was set to $T_s = 310\text{K}$ for the boundary condition of the energy equation, and the traction-free condition was applied along the boundary Γ_h for the momentum and energy equations. The temperature distribution of the paper disk, having been obtained from a linear interpolation of the experimental data shown in Fig. 3 [3], was treated as a function of time, and so the temperature of the paper disk was fixed anew at each time step. As for the initial conditions of the energy equations, the temperatures of the body and the air were set at 310K and 300K, respectively. The dimensions of the computational domain are given in Table 1, and the material properties of the skin, paper disk and air are summarized in Table 2.

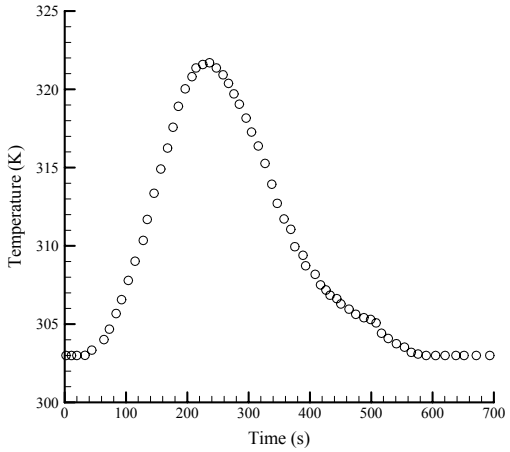

Fig. 3. Temperature history of paper disk of commercial moxa [3].

3. Numerical results and discussion

According to the study by Habash et al. [9], the effective temperature range for thermal stimulation is 40 - 50℃. Severe skin-burn or coagulation occurs above 50℃, and no thermal stimulation can be effected below 40℃. Therefore, in the present unsteady numerical simulations, the effective temperature range was monitored during the entire moxibustion process. Fig. 1 shows a schematic of the indirect moxibustion studied in the work of Lee et al. [3]. The moxa, which burns to ashes after combustion, is of cylindrical shape and mounted on a compressed paper disk with a hole in its center. In their experiment, the disk's temperature variation with time was obtained using a thermo-couple, as shown in Fig. 3. However, the data of the thermal stimulation inside the patient's skin tissue went unreported, since the temperature history there was not measured. Fig. 3 shows that the temperature of the paper disk increased due to the combustion of the moxa, after which, upon the combustion's completion, it cooled. In the present unsteady numerical simulations, the temperature history in Fig. 3 was used as the Dirichlet boundary condition for the whole paper disk.

According to Lee et al. [3]'s experimentation, the temperature difference between the center and the perimeter of the paper disk is relatively small for the entire duration of moxibustion, except that the maximum temperature difference is, approximately, less than 10% near the peak-temperature region. Therefore, in the present study, a uniform disk temperature was assumed.

Four widths of paper disk were tested in investigating the size effect. Since natural convection in the air zone is coupled with conduction in the moxa and in the body zone, the conjugate heat transfer was studied. The Rayleigh number of the natural convection was estimated using the data listed in Tables 1 & 2 and shown in Figs. 2 & 3:

$$Ra = \frac{g\beta(T_s - T_\infty)L^3}{\nu\alpha} \sim 10^5 \quad (4)$$

Table 1. Dimensions of computational domain.

$W(mm)$	$H(mm)$	$L_1(mm)$	$L_2(mm)$	$L_3(mm)$
6	3	100	50	100
9				
12				
18				

Table 2. Material properties of air, skin and paper disk.

Material	Density (kg/m^3)	Specific heat ($j/kg \cdot K$)	Thermal conductivity ($w/m \cdot K$)
Air	1.225	1006.43	0.0242
Skin	1000	4200	0.35
Paper	930	1340	0.18

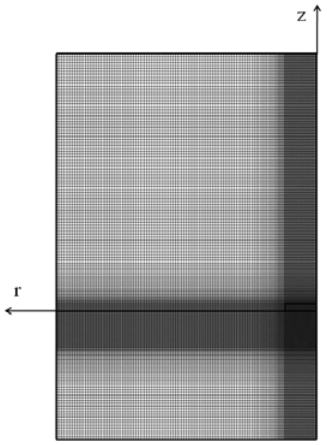

Fig. 4. Non-uniform mesh for computational domain (W=12 mm).

As given in Eq. (4), the maximum Rayleigh number of the natural convection was approximately 10^5, where β, ν and α represent the volume coefficient of expansion, the kinematic viscosity and the thermal diffusion coefficient of the air, respectively, for $L = 0.036\ m$ and $T_s = 321\text{K}$. Therefore, turbulence modeling was not included in this simulation [10]. Fig. 4 shows the non-uniform mesh applied to the conjugate heat-transfer problem.

The temperature histories with time for various grid resolutions with the time step of 0.04 sec were obtained at $(r,z) = (0,-5mm)$, as shown in Fig. 5, in order to find a grid-independent solution for the paper disk of 6 mm width. The results showed that a grid-independent solution can be obtained using an 85×169 non-uniform grid.

The temperature histories with time for various time steps were obtained at $(r,z) = (0,-5mm)$, as shown Fig. 6, in order to find a time step- and grid-independent solution to the unsteady conjugate heat-transfer problem.

That solution was found, in fact, for time steps smaller than 0.04 sec. Tables 4 and 5 show the relative errors of the maximum temperature difference at $(r,z) = (0,-5mm)$ for the various grid resolutions and time steps.

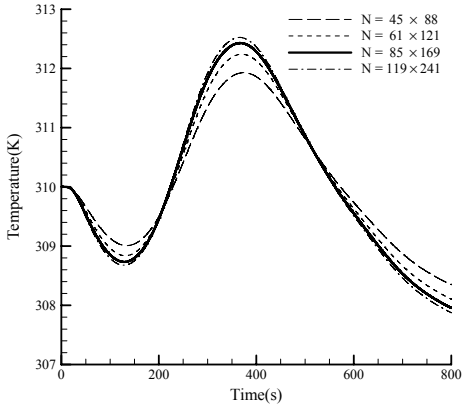

Fig. 5. Temperature history at $(r,z)=(0,-5mm)$ for various grid resolutions.

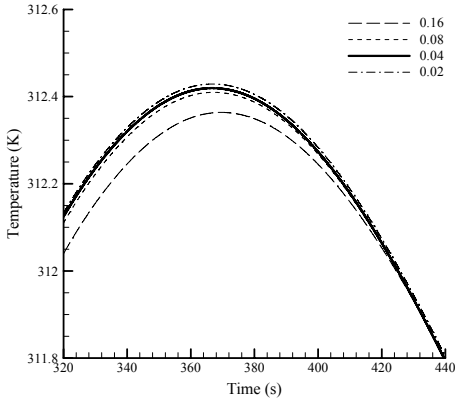

Fig. 6. Temperature history at $(r,z)=(0,-5mm)$ for various time steps.

The unsteady temperature distribution inside the body is an important factor in thermal stimulation. Despite this fact, as pointed out in the introduction, the relevant previous studies did not report this. The main purpose of the present numerical study was to examine the unsteady temperature field in moxibustion by way of solving the conjugate heat-transfer problem. Fig. 7 plots the temperature histories with time at $(r,z)=(0,-4mm)$ and $(r,z)=(0,-10mm)$ for the three widths (6 mm, 12 mm, 18 mm) of paper disk. It should be noted that the open circles in Fig. 7 represent the skin temperature, whereas in Fig. 3 they indicate the moxa temperature. It was found that the wider the paper disk is, the longer the effective stimulation period is. Fig. 8 reveals that the effective stimulation periods, in which the temperature is above 313K, are 241 sec for the paper disk of 6 mm and 263 sec for that of 12 mm.

The effective stimulation period was obtained by measuring the period in which the maximum temperature of the skin is higher than 313 K. The effective stimulation periods for the various widths of paper disk are shown in Table 3. As can be seen, the effective stimulation lasts longer for the wider paper disks.

Fig. 9 plots, for the four widths of paper disk, the maximum

Table 3. Effective stimulation periods for four widths of paper disk.

W (mm)	Duration time (s)
6	241
9	258
12	263
18	265

Table 4. Relative error of maximum temperature difference at $(r,z)=(0,-5mm)$ for various grid resolutions.

Grid resolution	45×88	61×121	85×169	119×241
Maximum temperature(K)	311.929	312.241	312.429	312.524
Relative error(%)	0.19	0.091	0.03	0

Table 5. Relative error of maximum temperature difference at $(r,z)=(0,-5mm)$ for various time steps.

Time step	0.32	0.16	0.08	0.04	0.02
Maximum temperature (K)	312.364	312.41	312.419	312.429	312.455
Relative error (%)	0.03	0.0144	0.0113	0.0083	0

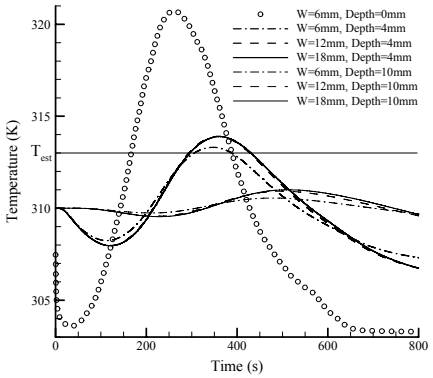

Fig. 7. Temperature history at $(r,z)=(0,-4mm)$ and $(r,z)=(0,-10mm)$ for three disk sizes.

temperatures along the depth (z) axis during the entire simulation (one cycle of moxibustion). Whereas the effective stimulation zone is larger, and the stimulation lasts longer, for the wider paper disks as shown in Table 3, the depth of the effective stimulation zone is saturated at approximately 5 mm.

Therefore, a 12 mm wide paper disk is recommended for the moxibustion (temperature history) used in the experimental study of Lee et al [3]. The unsteady temperature distributions inside the body, at six selected instants for the 6 mm paper disk, is plotted in Fig. 10. The temperature of the dermis falls lower than 310 K (body temperature) at 128 sec, since the initial temperature of the paper disk was set to 300 K (room temperature). The temperature of the disk increases as the combustion of moxa continues and the effective stimulation zone becomes larger accordingly, as shown in Figs. 10(b)~(d). The temperature of the paper disk reaches the body tempera-

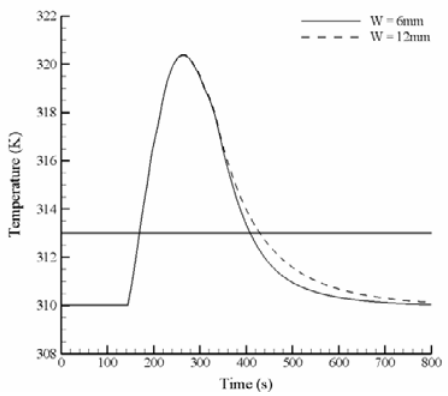

Fig. 8. Evolution of maximum temperature in skin for two disk sizes.

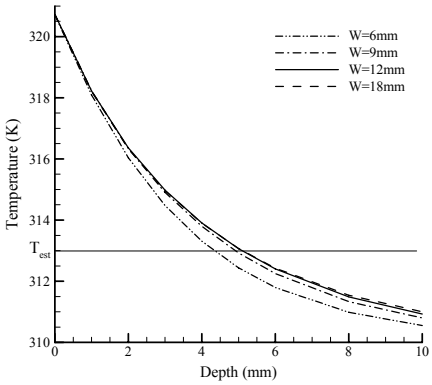

Fig. 9. Maximum temperature profiles along depth (z-) axis during one cycle of moxibustion for four widths of paper disk.

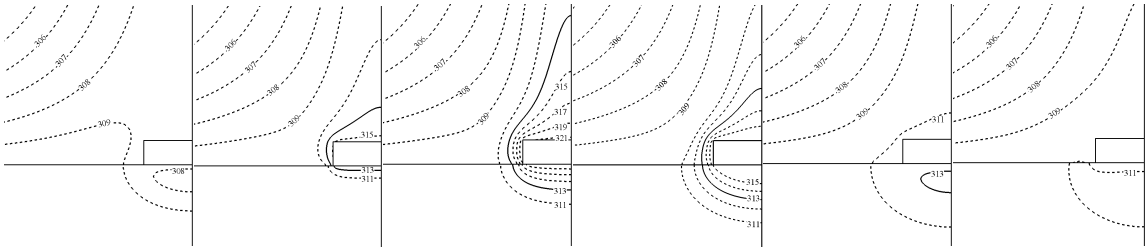

(a) 128s (b) 180s (c) 260s (d) 352s (e) 400s (f) 436s

Fig. 10. Evolution of temperature field inside body at six selected instants for paper disk of 6 mm.

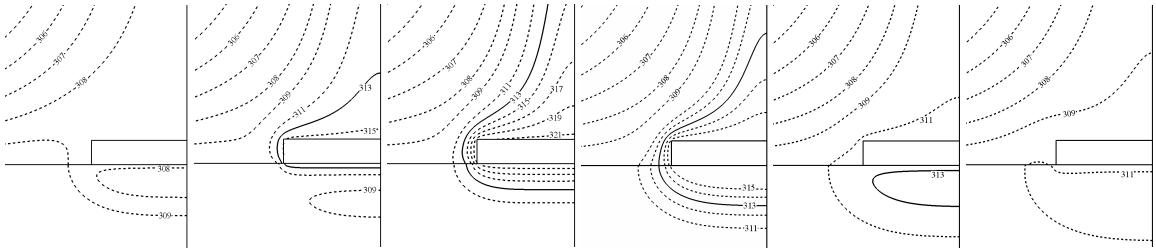

(a) 128s (b) 180s (c) 260s (d) 352s (e) 400s (f) 436s

Fig. 11. Evolution of temperature field inside body at six selected instants for paper disk of 12 mm.

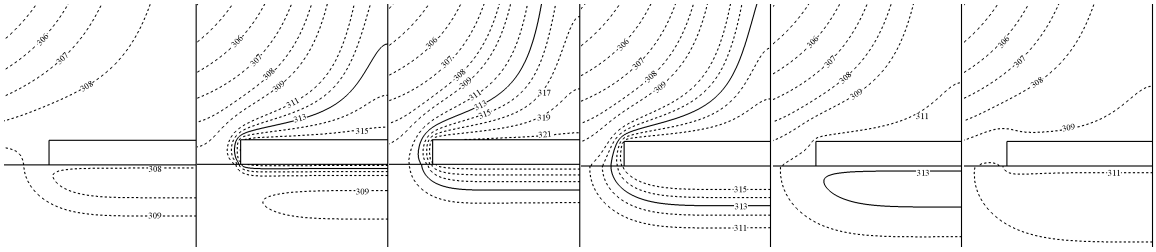

(a) 128s (b) 180s (c) 260s (d) 352s (e) 400s (f) 436s

Fig. 12. Evolution of temperature field inside body at six selected instants for paper disk of 18 mm.

ture (310K) at 128 sec, and the temperature of the dermis begins to rise above the body temperature at 180 sec. At 260 sec, the paper disk reaches the maximum temperature by moxibustion and the maximum depth of the effective stimulation zone is attained at around 352 sec, after which the temperature of the paper disk cools to the ambient temperature (300K). The effective stimulation temperature ($T_{est} = 313$ K) is plotted with a thick solid line in Fig. 10. The similar temperature distributions inside the body are plotted in Figs. 11 & 12 at six selected instants for the disk widths of 12 mm and 18 mm.

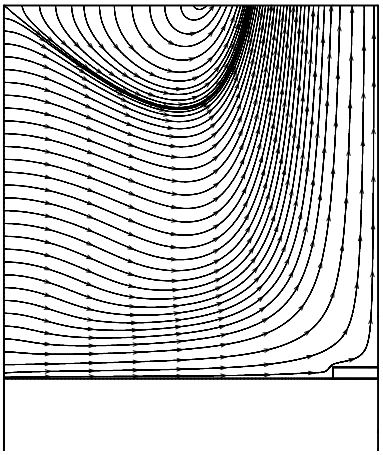

Fig. 13. Streamlines at near-maximum stimulation (w=12 mm, time= 352 sec).

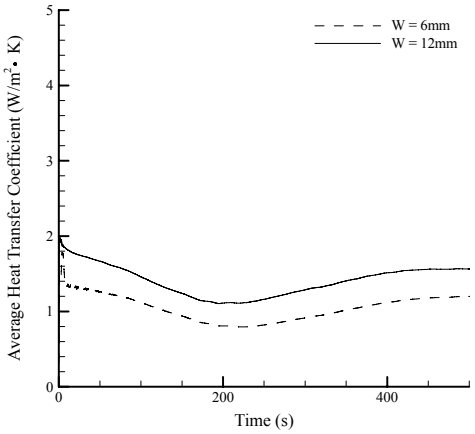

Fig. 14. Time variation of spatially averaged heat-transfer coefficient during entire simulation.

The trends are similar to those of Fig. 10. However, the effective stimulation zone becomes larger during the cooling period, as shown in Fig. 10(e), Fig. 11(e) and Fig. 12(e). It should also be pointed out that the difference of the depth of the effective stimulation zone between the 12 mm wide disk and the 18 mm one is trivial, as indicated in Fig. 11 and Fig. 12, though the effective stimulation zone naturally is larger with the wider disk. Fig. 13 shows the streamlines obtained at near-maximum stimulation revealing clearly that the body is cooled by the incoming cold fluid. Lastly, Fig. 14 plots the time variation of the spatially averaged heat-transfer coefficient during the entire simulation. The spatially averaged heat-transfer coefficient is between 0.8 and 2.0 $W/m^2 \cdot K$, and has a local minimum value near the time of maximum stimulation.

4. Conclusions

In the present study, a conjugate heat-transfer problem in indirect moxibustion was analyzed by solving the problem of convective heat transfer coupled with conductive heat transfer. The temperature history measured in [3] was linearly interpolated and used as the temperature boundary condition of the unsteady conjugate heat transfer. The grid- and time step-independent solution was obtained by testing various time steps and mesh resolutions. The effective stimulation periods for the four widths of paper disk were determined from the temperature histories inside the body as extracted at various depth levels, which histories had not been utilized in the previous studies. From the unsteady numerical simulations, the following conclusions were drawn.

(1) The depth of the effective stimulation zone is approximately 5 mm for the temperature history provided in [3].
(2) The effective stimulation zone becomes larger and lasts longer for wider paper disks. However, in the case of disks wider than 12 mm, the depth of the effective stimulation zone is saturated at approximately 5 mm.
(3) The streamline pattern obtained at near-maximum stimulation clearly shows that the body is cooled by the incoming cold fluid.

Acknowledgment

This study was supported by a grant of the Oriental Medicine R&D Project, Ministry for Health & Welfare & Family Affairs, Republic of Korea (B090040).

Nomenclature

K : Kelvin temperature
℃ : Celsius temperature
g : Gravity acceleration
Ra : Rayleigh number
r : Radial coordinate
z : Axial coordinate
T_{est} : Effective stimulation temperature
W : Width of paper disk
H : Height of paper disk
Γ_g : Dirichlet boundary condition
Γ_h : Traction-free condition
L : Length
N : Number of nodes
s : Time

Greek symbols

α : Coefficient of thermal diffusion
β : Coefficient of thermal expansion
ν : Kinematic viscosity

Subscripts

∞ : Ambient
a : Air
s : Skin

References

[1] J. K. Lim, Studies on Document of Moxibustion and Vital Reaction, *The Journal of Korean Oriental Medicine*, 13 (1976) 63-68.

[2] Y. S. Cheon, Y. S. Kim, J. D. Lee, D. Y. Choi, Y. B. Park, H. K. Koh, B. C. Ahn, D. S. Park, S. K. Kang, C. H. Kim and Y. H. Lee, The Experimental Study on Combustion Characteristics of the Moxa-Combustion in the Skin Model Agar, *The Journal of Korean Acupuncture & Moxibustion Society*, 16 (1999) 155-177.

[3] G. H. Lee, G. M. Lee and Y. J. Hwang, Experimental Study on the Thermodynamic Characteristics of Commercial Small-size Moxa Combustion, *The Journal of Korean Acupuncture & Moxibustion Society*, 18 (2001) 171-187.

[4] G. M. Lee, Y. S. Yang and G. H. Lee, Experimental Study on the Stimulating Effect of Commercial Moxa Combustion through the Measurement of Temperature – Focused on Combustion time and temperature, *The Journal of Korean Acupuncture & Moxibustion Society*, 19 (2002) 114-127.

[5] G. M. Lee, G. H. Lee, S. H. Lee, M. B. Yang, G. D. Go, E. M. Seo, J. D. Jang and B. C. Hwang, Experimental Study on the Stimulating Effect of Commercial Moxa Combustion through the Measurement of Temperature – Focused on ascending temperature gradient and effective stimulating period, *The Journal of Korean Acupuncture & Moxibustion Society*, 19 (2002) 64-76.

[6] D. H. Bang, Y. B. Park and S. K. Kang, An Experimental Study of Moxa – Combustion Time in each Period by the Density of Moxa Material, *The Journal of Korean Acupuncture & Moxibustion Society*, 12 (1995) 243-251.

[7] Y. B. Park, S. K. Kang and W. Huh, An Experimental Study on the Characteristics of Moxa Combustion(II) – On the Density of Moxa Material, *Kyunghee University, Korea*. 17 (1994) 191-199.

[8] LIU Zhipeng, YIN Tao and LI Ying, Thermodynamics Model and Experimental Validating on Thermal Field Distribution of Traditional Moxibustion, *Engineering in Medicine and Biology 27th Annual Conference*, 5 (2005) 4951-4954.

[9] Riadh W. Y. Habash, Rajeev Bansal, Daniel Krewski, and Hafid T.Alhafid, Thermal Therapy, Part 1 : An Introduction to Thermal Therapy, *Critical Reviews in Biomedical Engineering*, 34 (2006) 459-489.

[10] J. P. Holman, *Heat Transfer,* McGraw-Hill, New York, USA (1986).

Byoung-jin Jeon is currently in the Masters course at Seoul National University of Technology. He is interested in the numerical simulation of various conjugate heat-transfer phenomena.

Hyoung-gwon Choi received a Ph. D at Seoul National University majoring in FEM-based computational fluid dynamics based on finite element method from Seoul National University. He is currently an associate professor of the Department of Mechanical Engineering of Seoul National University of Technology.